electronics

MDPI

Article

Unmanned Aerial Vehicle-Based Automated Path Generation of Rollers for Smart Construction

Hyung-Jin Kim, Jae-Yoon Kim, Ji-Woo Kim, Sung-Keun Kim and Wongi S. Na *

Department of Civil Engineering, Seoul National University of Science and Technology, Seoul 01811, Republic of Korea; hyungjin4843@seoultech.ac.kr (H.-J.K.); 17100709@seoultech.ac.kr (J.-Y.K.); gukim97@seoultech.ac.kr (J.-W.K.); cem@seoultech.ac.kr (S.-K.K.)
* Correspondence: wongi@seoultech.ac.kr

Abstract: The construction industry is continuously evolving, seeking innovative solutions to enhance efficiency, reduce costs, and improve safety. Unmanned aerial vehicles (UAVs), commonly known as drones, have emerged as a transformative technology in the construction sector, offering numerous advantages in data collection and site management. This paper presents a novel approach for utilizing UAVs to automate the path generation of rollers, a crucial element in the construction of roads and other large-scale infrastructure projects. A UAV was used to scan the target area to create a model; the next step was to generate the path for the rollers. Traditionally, the process of determining optimal roller paths is labor-intensive and reliant on manual surveys and engineering expertise. This study proposes a streamlined workflow that harnesses UAVs equipped with computer vision technology to capture high-resolution topographical data of construction sites. This data is then processed through an algorithm created by the authors that automatically generates optimized roller paths based on several factors.

Keywords: UAV; drone; aerial inspection; smart construction; path generation

Citation: Kim, H.-J.; Kim, J.-Y.; Kim, J.-W.; Kim, S.-K.; Na, W.S. Unmanned Aerial Vehicle-Based Automated Path Generation of Rollers for Smart Construction. *Electronics* **2024**, *13*, 138. https://doi.org/10.3390/electronics13010138

Academic Editors: Yunda Yan, Dewei Yi, Hao Lu and Lan Gao

Received: 6 November 2023
Revised: 26 December 2023
Accepted: 26 December 2023
Published: 28 December 2023

1. Introduction

The current construction industry is facing a shortage of skilled workers due to the aging workforce of construction professionals and a decreasing influx of new talent. This situation necessitates resolving the skilled worker shortage issue and enhancing the industry's competitiveness. These challenges are common worldwide, and many countries are implementing various policies to apply and develop new technologies emerging from the Fourth Industrial Revolution in the construction industry. One possible suggestion to overcome the aforementioned problem could be to use drones at the construction stage.

Research has been conducted to address the issues in earthwork operations by applying smart construction technology to traditional methods. One of the most prevalent research areas focuses on utilizing machine guidance (MG)/machine control (MC) systems to conserve human and material resources to improve the efficiency of operations. A notable study by Park et al. compared the time and accuracy required for excavators equipped with MG/MC systems and standard excavators without any attachments to work on the same cross section under identical conditions [1]. The accuracy of MG/MC systems was consistently higher than the conventional methods, and the time required was also shorter. Furthermore, the study demonstrated that MC systems, which enable the equipment's free movement through attachments, achieved the highest level of accuracy. There are also preliminary studies aimed at reducing accidents during equipment operation [2–4]. Most fatal accidents in construction work are related to equipment. Therefore, research has been conducted to monitor the real-time location of equipment or predict the working space of equipment to prevent collisions between equipment or to prevent workers from entering hazardous areas [5].

Additionally, systems that differentiate between equipment and workers using deep learning and algorithms, and provide alerts based on the distance between them, have been developed. These systems have gained recognition for their safety features and are being utilized in the field in both detachable and integrated forms.

While various studies have been conducted to improve work safety and efficiency through research on equipment-related aspects and the attachment of new sensors or equipment, there is a significant lack of research that directly generates equipment paths. A similar case in the realm of Fourth Industrial Revolution technologies involves the use of unmanned aerial vehicles (UAVs), where research on path generation algorithms is being conducted and widely applied across various industries. Notable algorithms used in UAV path generation include genetic algorithm (GA), particle swarm optimization (PSO), and ant colony optimization (ASO) [6]. The common goal of this research is to generate flight paths that satisfy the necessary conditions and constraints for flight while passing through specified starting and target points using computational intelligence (CI). In essence, it involves utilizing the UAV's fast processing capabilities and a series of data with information about the characteristics of UAV movement to continuously provide an optimized path until it meets the desired conditions of the operator [7–9]. Furthermore, Aggarwal et al. classified three types of techniques: representative techniques, collaborative techniques, and non-cooperative techniques, and compared and analyzed studies related to the path planning of UAVs with variables such as cost, time efficiency, and path length [10]. Cho et al. proposed cell decomposition, which divides the flight range of UAVs into hexagons, and developed a MILP (mixed-integer linear programming) model that reduces the time it takes for UAVs to navigate the region [11]. Kyriakakis et al. similarly tried to develop algorithms that minimize the time it takes for UAVs to fly over all specified ranges. They used the same cell decomposition as previous studies and implemented the GRASP-VND (greedy randomized adaptive search procedure—variable neighborhood descent) algorithm [12]. Zammit et al. also conducted a study to identify the cause, define different path scenarios, and verify their performance using A* and RRT algorithms to solve the problem of UAVs having to fly in real time in an environment with high uncertainty [13].

Path generation research using UAVs is traditionally based on utilizing nodes or dividing the intended flight space into grids. However, directly applying this approach to construction sites where earthwork operations occur can be challenging. The terrain is often not perfectly linear, leading to areas that cannot be covered by a grid, and the elevation of earth and sediment can vary significantly, posing difficulties for equipment operation. Currently, the paths followed by equipment in construction sites are often subject to the judgment of the operators. In such cases, variations in operator skill can lead to differences in the quality of work even when working on the same section. Therefore, there is a need for research that can update site information in real time and guarantee consistent quality through path generation.

The significance of path generation research has been consistently emphasized over time, with research efforts encompassing various aspects. Kim et al. conducted research in large construction equipment path planning, with a particular emphasis on path visualization. Their approach involved dividing the construction site into cells and proposing cost-effective paths based on five factors: workload, distance, slope, complaints, and others [14]. Hirayama et al.'s research focused on analyzing the characteristics of bulldozer blades and accounting for variations in bulldozer speed when planning paths [15]. Ghadamid et al. conducted research in UAV path generation, utilizing the genetic algorithm (GA) to optimize routes for waste collection trucks [16]. Li and Rao et al. contributed to bulldozer path generation research by proposing a BINN hybrid algorithm-based CCPP approach, which included designing a framework for bulldozers with autonomous path planning capabilities [17].

Historically, path generation research for earthwork equipment, much like UAV research, involved methods such as cell decomposition or combinations of earth and sediment to create paths connecting entrances and exits. However, these methods often assumed

constant equipment paths and analyzed movements based on equipment workload. Given the dynamic nature of construction sites with various objects constantly in motion, these approaches have limitations. Therefore, there is a need for path generation methods that consider specific work patterns, allowing for combinations of straight and reverse movements. Additionally, integrating equipment path generation algorithms is crucial.

In this research, a methodology was proposed to automatically generate work paths using UAVs for rollers, which is a relatively new area of research in this field. UAVs allow not only for terrain exploration but also for the analysis of earth and sediment. Three key advantages can be gained by applying UAVs in this study. Firstly, it enables faster scanning of extensive construction sites, increasing efficiency. Secondly, it provides high-resolution images and data using GPS and sensor technology. Lastly, the most crucial point is the real-time monitoring capability. Given the high variability of construction sites, it is essential to assess the situation before deploying equipment or workers. Utilizing UAVs allows for the rapid detection of on-site conditions and provides opportunities for addressing issues promptly. This study uses a UAV to scan the site where the equipment is to be deployed and generates CAD drawings with terrain information through Pix4D. Based on the drawings, a path for the roller to perform the earthwork is planned, which, unlike previous earthwork equipment path studies, covers the entire working area and is customized to the work characteristics. Any changes to the site can be re-scanned using the UAV to update the BIM model in real time with the Pix4D program for generating an efficient path for the rollers.

2. Rollers

Rollers are equipment used to compact materials such as loose soil, asphalt pavement on roads, gravel, and crushed-stone pavement. They compact these materials to increase density, enhancing shear strength and bearing capacity. Different types of rollers are used depending on the specific work requirements, which can be seen in Figure 1. The concept of automatic path generation introduced in this study would be suitable for all roller types during the construction stage.

Figure 1. Three different types of rollers for construction.

When conducting compaction operations with a roller, it is crucial to select the appropriate compaction equipment based on factors like construction duration, processes, construction costs, soil conditions, and on-site conditions. Compaction work is typically carried out longitudinally, following the length of the soil stack. It starts from the side (outermost line) and sequentially proceeds toward the center, using the roller's back-and-forth movement until the specified compaction density is achieved. The typical number of repetitions ranges from 8 to 20. Rollers have one of the simplest work patterns among earthwork equipment. They perform their tasks by repeatedly moving forward and backward until they meet the specified compaction requirements or compaction density. Rollers do not require separate work zone divisions and are deployed to areas where graders or dozers have completed their work. Additionally, unlike graders or dozers, rollers do not need to

consider the movement of attachments. The drum of the roller only moves in the direction of equipment advancement, making the path generation process relatively straightforward. One can understand the work pattern of rollers through Figure 2. As seen in the upper left corner of the legend, rollers follow the yellow line while advancing. When they reach a checkpoint, typically determined by the maximum forward distance or the judgment of the operator, they reverse along the red line and then turn to advance again. In this study, the rightmost yellow line serves as the reference for creating the work area.

Figure 2. General movement of roller at construction site.

3. Automation of Roller Path Generation

3.1. UAV-Based BIM Model Creation

To create a path for the rollers during the construction phase, we first needed a bird's-eye view of the construction site. To achieve this, a quadcopter-type DJI Mavic 2 was used, which is shown in Figure 3. It has a battery capacity of 3850 mAh and can reach a maximum speed of 72 km/h. It is capable of capturing images over a wide area, with a controllable range of up to 8 km. The overlap ratio and maximum altitude can also be configured through DJI's software (version 4.3.60). In this research, a maximum altitude of 80 m and overlap ratios of 70% for lateral overlap and 80% for longitudinal overlap were chosen to capture data with the highest precision possible. These values are usually set by experts in this field to acquire high-quality data efficiently, considering the short operating time of the UAV.

Using the UAV, a 3D BIM model of the construction site was created; this process is shown in Figure 4. First, the ground control points (GCPs) were measured (Figure 4a). Once these points were set, the UAV flew over the area to acquire images, as shown in Figure 4b, where point cloud coordinates were generated with X, Y, and Z values with reference to the GCPs. Images were processed using the Pix4D Mapper program, shown in Figure 4c, where they were then transformed into a 3D BIM model, shown in Figure 4d. Since the purpose of the roller operation is to smooth out the surface at the construction site (Z-direction), we did not need to consider this for this study. Thus, only X and Y coordinates were used for path creation.

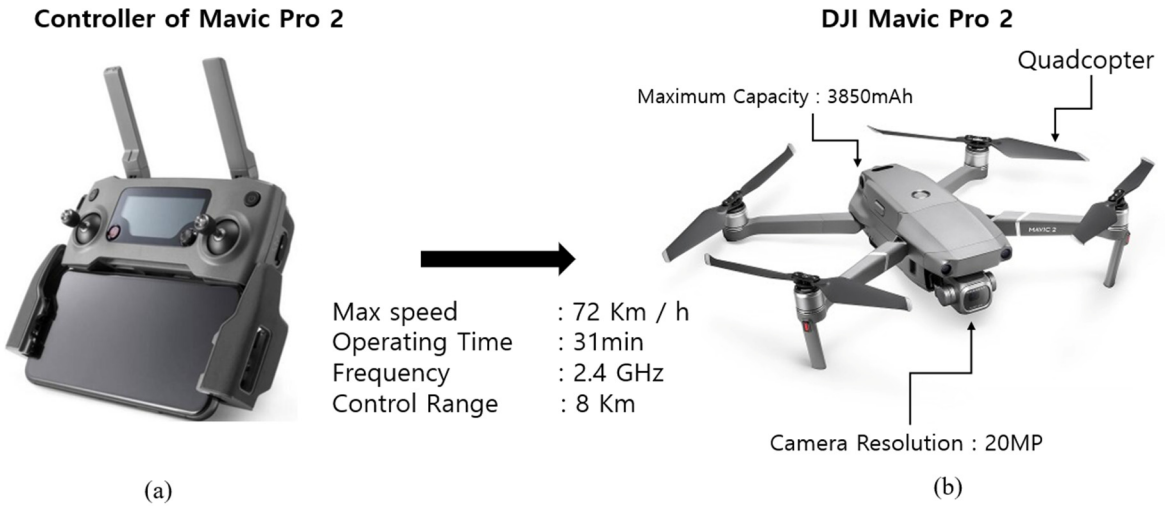

Figure 3. (**a**) Controller of UAV; (**b**) Photo of UAV used for the study (Mavic Pro 2).

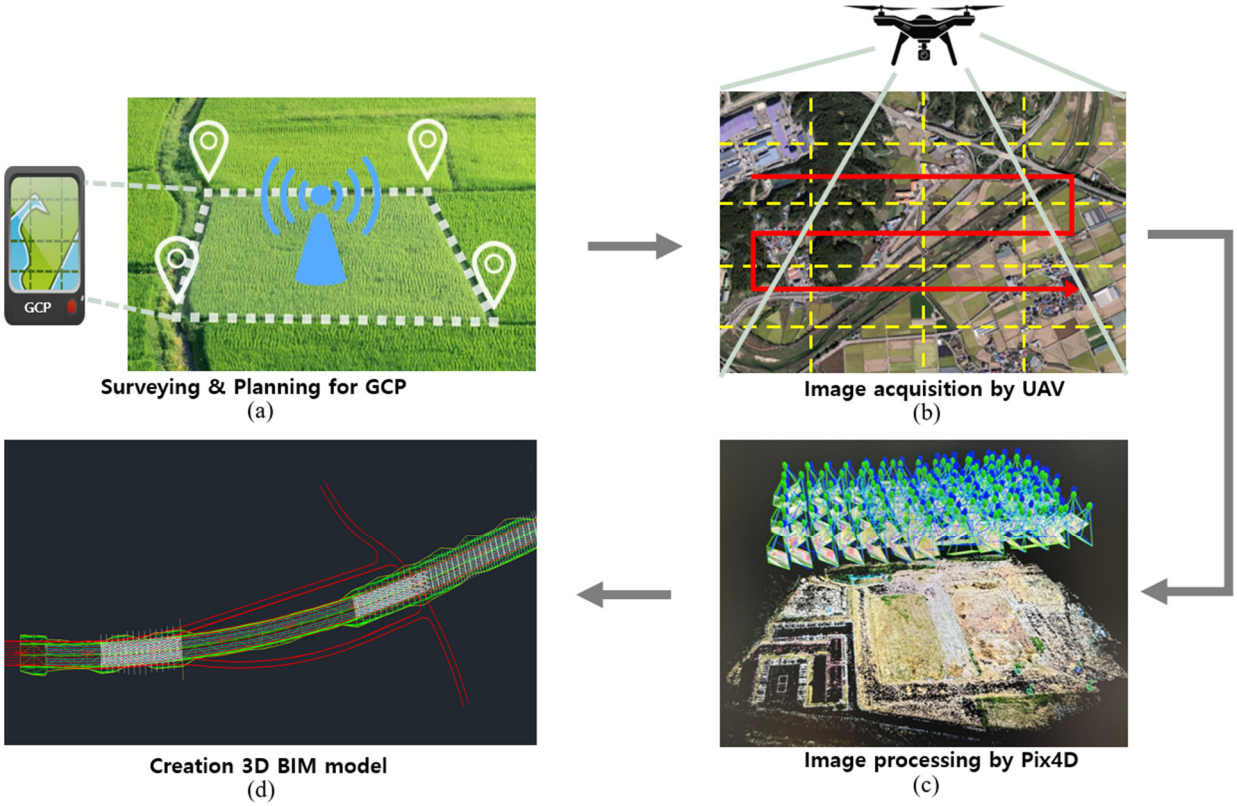

Figure 4. BIM model creation using UAV (**a**) aerial survey; (**b**) image acquisition; (**c**) image processing; (**d**) model creation.

3.2. Path Generation Process

In this study, a Python code-based algorithm was used for generating the operational planning path for the roller. After field scanning using a UAV, the work sections were determined and the parameter values were calculated. This section represents the entire process for generating the path for the roller for this work. A general understanding of this process can be obtained by referring to the flow chart in Figure 5. The figure illustrates the entire process of path generation, which is divided into three parts: (i), (ii), and (iii), as shown in the figure. The path generation process begins by creating a BIM model from the site captured by the UAV (which is the box with a red dotted line in (i)). The BIM model is

based on CAD drawings that contain all the information about the construction site, and the path is generated onto this BIM model. After selecting the working area from the BIM model, the next step is (ii), where the coordinates of the outermost lines of the selected work area are extracted and trend lines are generated based on these coordinates.

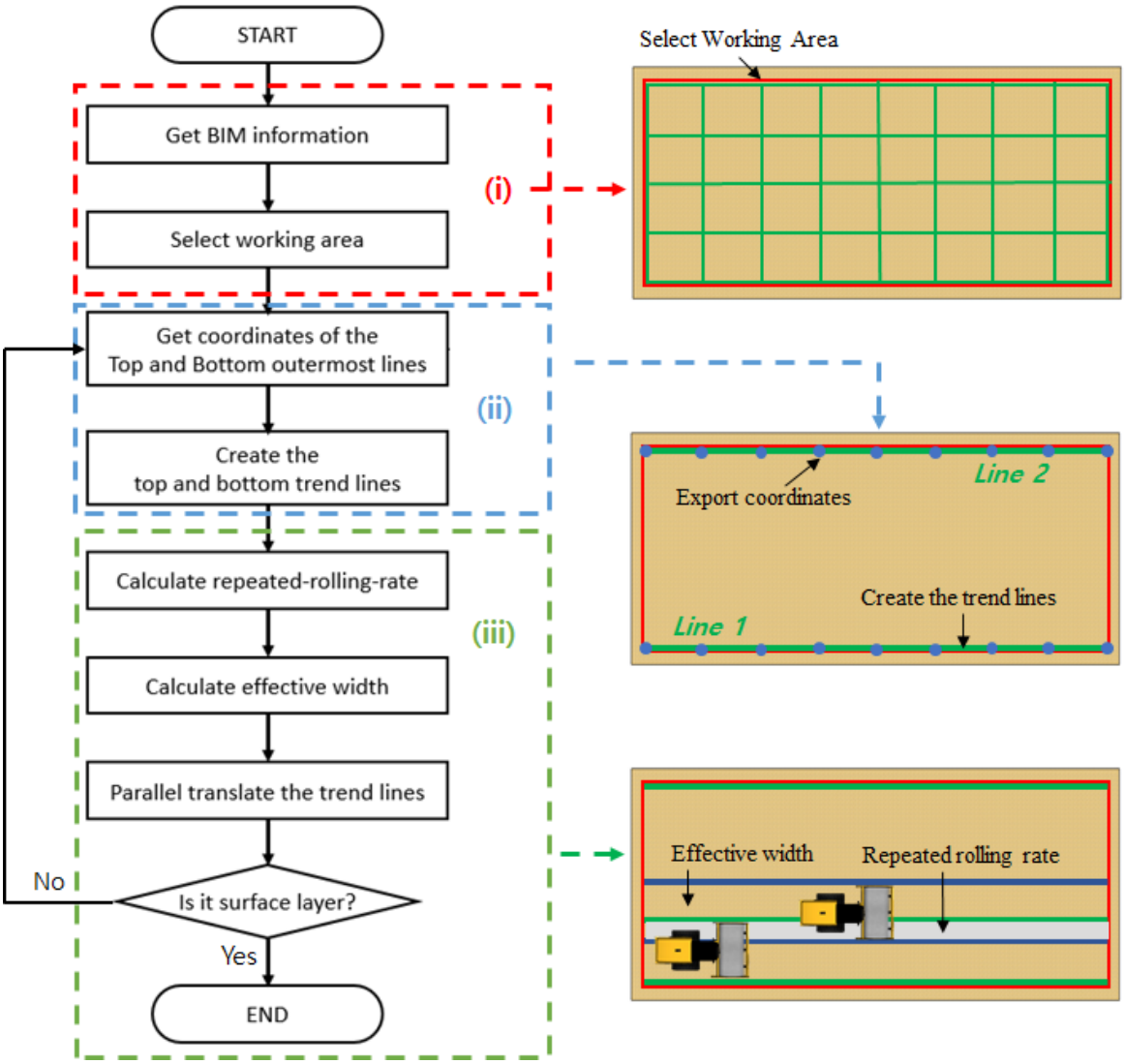

Figure 5. Flow chart of path generation automation using a UAV.

The sequence of this step is as follows: in the selected section of the construction area, the 'cexp' command is used to extract coordinates from the outermost two lines of the 3D BIM model, which are then saved in a CSV file. Each line consists of 70 coordinates. Assuming the road progresses from left to right, the path created in the forward direction from the lower node is defined as line1 (data1), and the path created from the upper node is defined as line2 (data2). To visualize the outermost working paths defined by Line 1 and Line 2 using Python code, it is convenient to align the y-axis with the equipment's working direction in a 2D plane. Therefore, the entire working line is rotated to always align the starting point with the y-axis parallel, using the slope of the line connecting the starting points of Line 1 and Line 2 and the 'atan' function.

The last part (iii) requires one to determine 'repeated rolling rate' and 'effective width' shown in Figure 5, where 'repeated rolling rate' is simply the overlapped area when the roller is traveling over the next path. Some studies [18,19], aimed at improving efficiency and reliability through roller operation monitoring, mentioned that repeated rolling is

a problem that needs to be addressed to enhance the quality of the work. To determine these factors, one study conducted interviews and surveys from a pool of experts in this field, including actual operators [20]. The survey participants consisted of a total of six individuals, with two having less than 20 years of experience, four having between 20 and 30 years of experience, and four having over 30 years of experience, as summarized in Figure 6. Based on the survey results, it was found that a repeated rolling rate of approximately 0.25–0.4 was suitable for the width of the working area. The effective width of the equipment is determined in the process of defining the repeated rolling rate. If the value between the paths is 1 and a repeated rolling rate is between 0.25 and 0.4, the effective width of the equipment naturally becomes the difference of two values.

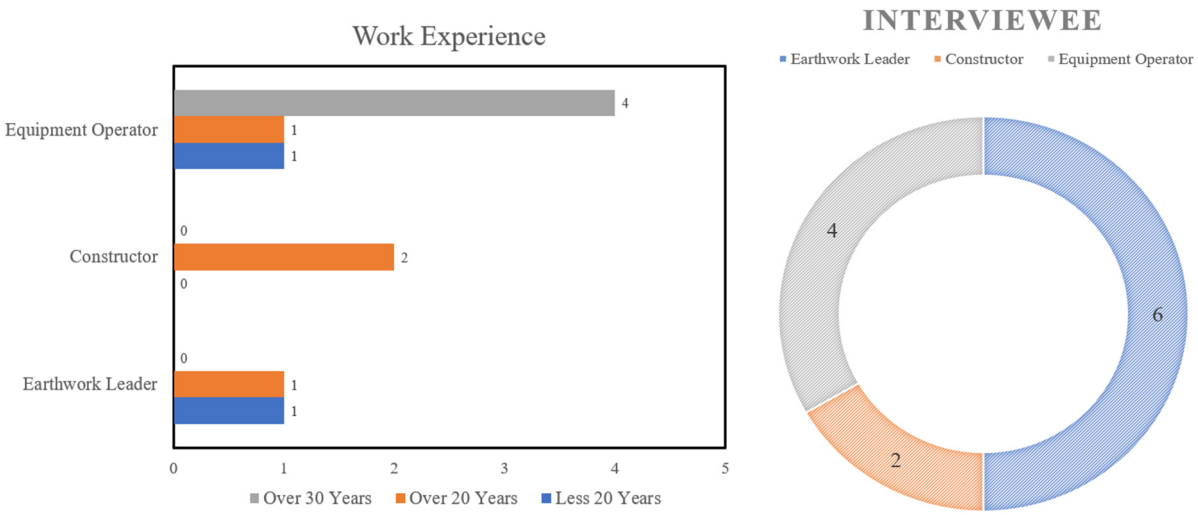

Figure 6. Work experience of surveyed experts.

After determining the path generation-related elements, the next step was to insert the necessary values into the Python code that the authors created, including the coordinates of the initially loaded outermost line, which are indicated in red (Figure 7). Outermost lines are colored in green, and the blue dotted lines are the actual path for the roller movement. This parallel trend line is also calculated from the created algorithm.

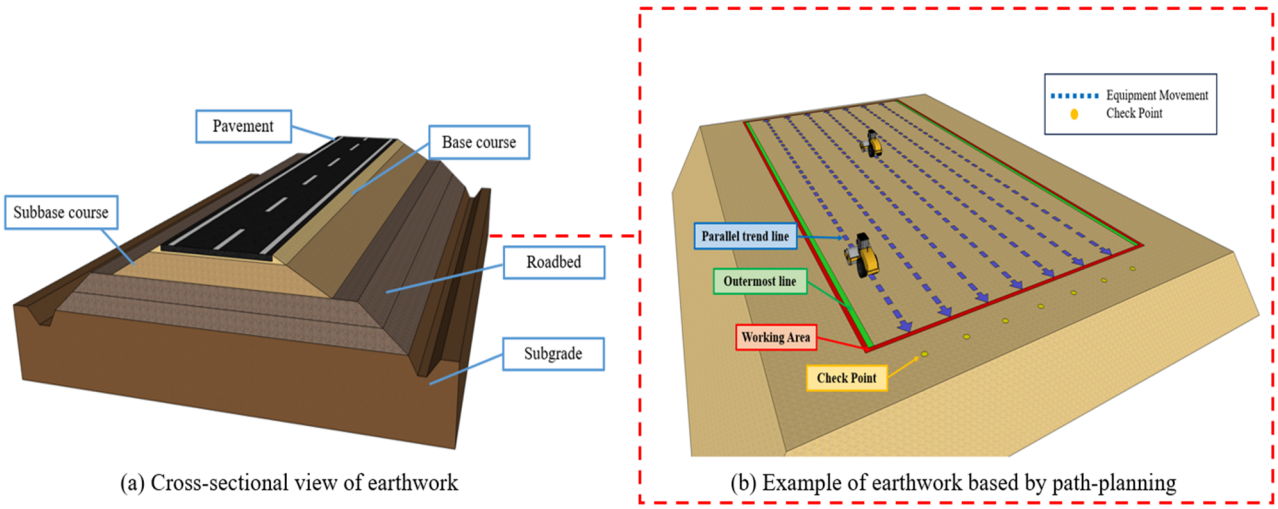

Figure 7. Visualization of path generation using the algorithm created with Python.

In this study, it was assumed that the roller performs forward and backward operations only within the selected work area. However, in cases where a single roller needs to perform

a single task and requires path changes, this can be addressed by extracting additional coordinates. The method involves moving to a checkpoint on the same line as each work line and then changing the path to the next line. Checkpoints are represented as yellow dots in Figure 7. The last step of path generation is to determine the equipment's deployment location. It involves checking whether the roller is operating on the pavement or on other layers such as the base course, roadbed, or subgrade. This is an essential process in the study. In the case of the pavement layer, there is a gentle slope for equipment safety, but the height remains unchanged after compaction. In contrast, the subgrade and base course layers are not the final construction surface, so the height increases by 30 cm and 20 cm, respectively, for each layer after compaction. As a result, as the height increases, the width of the work area narrows. This configuration is clearly evident in Figure 7. Therefore, when the work area is not on the pavement layer, it is necessary to revisit the process of obtaining the coordinates of the outermost line and repeat this process.

4. Case Study of a Construction Site in South Korea

In this study, a case study was conducted based on the design drawings of the inland expressway project being carried out in Jeungpyeong County, Chungcheongbuk-do, South Korea. Due to the nature of vehicle road characteristics, where the distinction between curves and straight sections is not always precise, two types of sections were chosen: straight and straight–curved mixed sections, as shown in Figure 8. This section was determined arbitrarily based on the information from the drawings. Additionally, fourth to eighth-degree polynomials were used as trend lines in the process of generating paths. The selected sections in the case study all targeted road sections with a width of 23 m and the length of the work area was set to 60 m, consistent with the roller's one-time working distance. The equipment targeted for roller work paths was assumed to have a width of 4 m, based on general roller specifications. Using these assumed values, the number of roller paths required and the repeating roller rate were determined as 8 and 0.33623, respectively. Using this concept, one could generate a path for rollers regardless of the shape of the construction site.

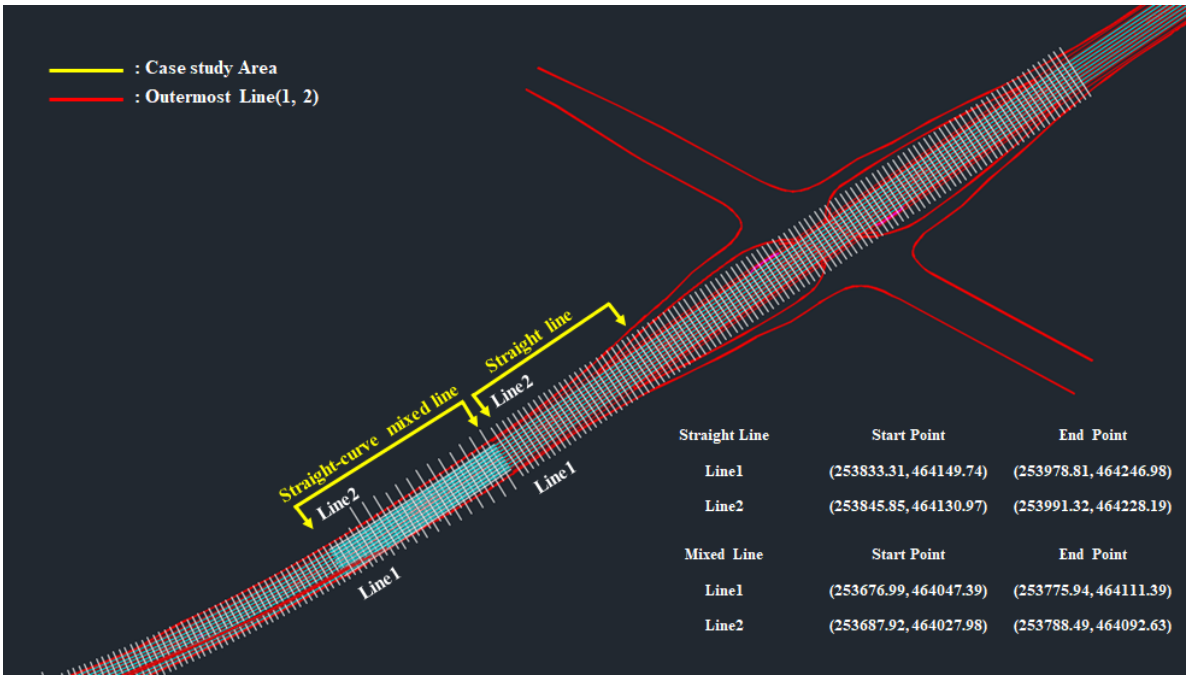

Figure 8. Target area for roller path generation in South Korea.

4.1. Straight-Line Section

In this section, the authors created five trend lines to automate the path of rollers to the 'straight line' section in Figure 8. These trend lines were created for 'Line 1' and 'Line 2'; the coordinates are labeled in the figure. For example, the trend lines created for 'Line 1' start at (x: 253,833.31, y: 464,149.74) and end at (x: 253,978.81, y: 464,246.98). Here, x and y values were used to create the trendlines shown in the table below.

The roller path trend lines generated based on the extracted coordinates for each line can be found in Table 1. As mentioned earlier, a total of 10 trend lines, ranging from fourth to eighth order, were created by distinguishing between top and bottom. From the equations, one can see that a constant value of 27.16 is observed for all equations for Line 2 (top) while the constant for Line 1 (bottom) changes from 0.0003692 to 0.0002216. This is expected due to the possibility of the construction site being not perfectly straight.

Table 1. Trend lines for the straight line section.

Grade of Trendline	**Line 1 (Bottom)**
4th	$-4.409e^{12}x^4 + 5.378e^{10}x^3 + 2.697e^8x^2 + 0.6683x - 0.0003692$
5th	$-1.725e^{13}x^5 + 5.828e^{11}x^4 - 7.53e^9x^3 + 4.616e^7x^2 + 0.6683x - 0.0003312$
6th	$2.698e^{14}x^6 - 1.194e^{11}x^5 + 1.997e^9x^4 - 1.567e^7x^3 + 5.792x^2 + 0.6683x - 0.0001106$
7th	$-2.6388e^{16}x^7 + 1.613e^{13}x^6 - 3.895e^{11}x^5 + 4.71e^9x^4 - 2.985e^7x^3 + 9.41e^6x^2 + 0.6682x - 0.0000334$
8th	$-1.853e^{17}x^8 + 1.051e^{14}x^7 - 2.391e^{12}x^6 + 2.775e^{10}x^5 - 1.72e^8x^4 + 5.363e^7x^3 - 6.596e^6x^2 + 0.6683x - 0.0002216$
Grade of Trendline	**Line 2 (Top)**
4th	$2.044e^{11}x^4 - 4.249e^9x^3 + 2.568e^7x^2 + 0.6683x + 27.16$
5th	$1.177e^{13}x^5 - 1.503e^{11}x^4 - 7.17e^{10}x^3 + 1.28e^7x^2 + 0.6683x + 27.16$
6th	$-5.24e^{15}x^6 + 2.009e^{12}x^5 - 2.606e^{10}x^4 + 1.274e^8x^3 - 1.275e^7x^2 + 0.6683x + 27.16$
7th	$-3.79e^{16}x^7 + 1.54e^{13}x^6 - 2.355e^{11}x^5 + 1.637e^9x^4 - 4.943e^8x^3 + 3.965e^7x^2 + 0.6683x + 27.16$
8th	$1.032e^{17}x^8 - 5.348e^{15}x^7 + 1.096e^{12}x^6 - 1.117e^{10}x^5 + 5.75e^9x^4 - 1.283e^7x^3 + 3.439e^7x^2 + 0.6684x + 27.16$

4.2. Straight–Curved Mixed Line

In this section, another set of 10 trend lines was created for the 'straight–curved mixed line' section of Figure 8. Again, the coordinates for 'Line 1' and 'Line 2' are shown in the figure and the trend lines are shown in Table 2. Here, a similar pattern is observed for the constants, where one can see that a constant of value 26.4 is observed for all equations for Line 2 (top), while the constant for Line 1 (bottom) changes from 0.00006987 to 0.0005632.

Figure 9 shows the final stage of our study, where the BIM model is combined with the algorithm to show the path for the rollers. One can say that with the algorithm created in this study, it is possible to automate a path for rollers for various construction sites with different curves. In the next section, the errors regarding this technique are analyzed in detail.

4.3. Error Analysis of Trend Lines Compared to Construction Site

It is crucial to analyze the errors between the actual site's drawings and the trend lines generated based on coordinates to determine whether this method exhibits sufficient accuracy for real-world applications. The coordinates used in the case study reflect complete field information, but the trend line created based on the coordinates may not completely cover the field due to inflection points or order changes due to the nature of the formula, which may cause errors. Therefore, additional code was written in Python to analyze errors and is analyzed in this section.

Table 2. Trend lines for the straight–curved section.

Grade of Trendline	Line 1 (Bottom)
4th	$-1.899e^{9}x^{4} - 1.562e^{6}x^{3} + 0.0006219x^{2} + 0.598x + 0.0006987$
5th	$-1.725e^{13}x^{5} + 5.828e^{11}x^{4} - 7.53e^{9}x^{3} + 4.616e^{7}x^{2} + 0.6683x - 0.0003312$
6th	$-5.71e^{13}x^{6} + 1.857e^{10}x^{5} - 2.49e^{8}x^{4} - 2.185e^{7}x^{3} + 0.0005851x^{2} + 0.5984x - 0.0002191$
7th	$1.195e^{14}x^{7} - 4.781e^{12}x^{6} + 7.707e^{10}x^{5} - 6.547e^{8}x^{4} + 1.242e^{6}x^{3} + 0.0005595x^{2} + 0.5986x - 0.0004494$
8th	$-2.629e^{16}x^{8} + 1.177e^{13}x^{7} - 2.212e^{11}x^{6} + 2.257e^{9}x^{5} - 1.365e^{7}x^{4} + 3.104e^{6}x^{3} + 0.0005351x^{2} + 0.5987x - 0.000563$
Grade of Trendline	**Line 2 (Top)**
4th	$-7.534e^{10}x^{4} - 1.952e^{6}x^{3} + 0.0005902x^{2} + 0.6115x + 26.4$
5th	$6.682e^{11}x^{5} - 1.362e^{8}x^{4} - 1.154e^{6}x^{3} + 0.0005744x^{2} + 0.6115x + 26.4$
6th	$-5.012e^{12}x^{6} + 1.222e^{9}x^{5} - 1.069e^{7}x^{4} + 1.811e^{6}x^{3} + 0.0005521x^{2} + 0.6112x + 26.4$
7th	$2.084e^{13}x^{7} - 6.097e^{11}x^{6} + 6.792e^{9}x^{5} - 3.52e^{7}x^{4} + 5.842e^{6}x^{3} + 0.0005616x^{2} + 0.6106x + 26.4$
8th	$-5.232e^{15}x^{8} + 1.811e^{12}x^{7} - 2.508e^{10}x^{6} + 1.749e^{8}x^{5} - 6.254e^{7}x^{4} + 7.501e^{6}x^{3} + 0.0005992x^{2} + 0.6103x + 26.4$

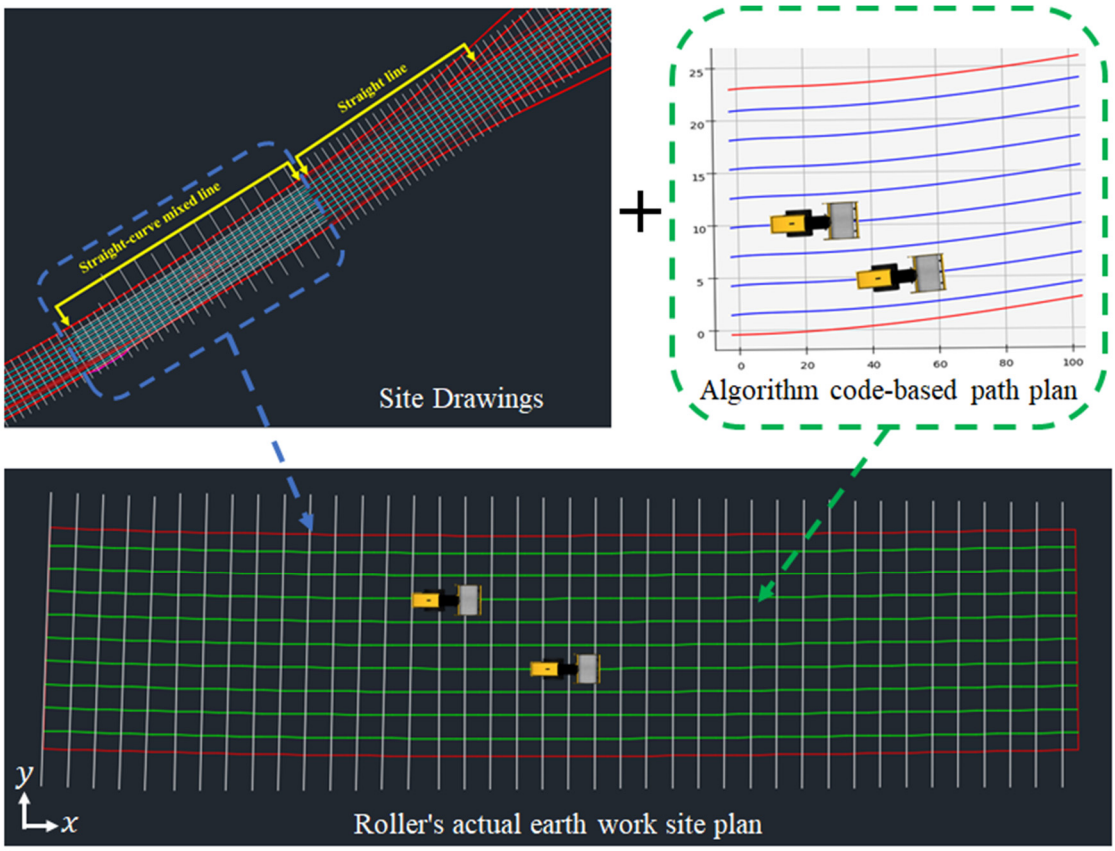

Figure 9. Generated path for rollers.

The process of analyzing errors is simple. Since the extracted coordinates are actual site drawing information, comparing them with the generated trendline indicates the accuracy. Like the path generation, the error analysis algorithm is also based on Python code. The code proceeds as follows: first, as with path generation, the extracted coordinates need to be saved in a CSV file and loaded with the data to be used. The saved CSV file is the same one used in the previous path generation. Next, after entering the order of the trend line to be analyzed, a path identical to that of Tables 1 and 2 is generated. By

substituting the x-coordinate values of the saved CSV file into the generated trendline, the y-values of the trendline are obtained. This value is defined as the predicted y-value from the trendline and is saved using the command trend_y_predicted. Finally, by calculating the difference between the y-values in the CSV file (drawing-extracted y-values) and the predicted y-values from the trendline, errors can be computed. In this study, as the path generation is divided into top and bottom lines, errors were stored separately for each line as error1 and error2. The largest error is output when all x-values are substituted and calculated. All calculated errors were based on absolute values, and the unit is in meters.

Figure 10 shows the errors calculated between the actual site and the trend lines created for the study. In both straight and straight–curved mixed lines, the bottom of the section is indicated in blue, while the top is indicated in green. The average of the top and bottom lines' errors is indicated in yellow.

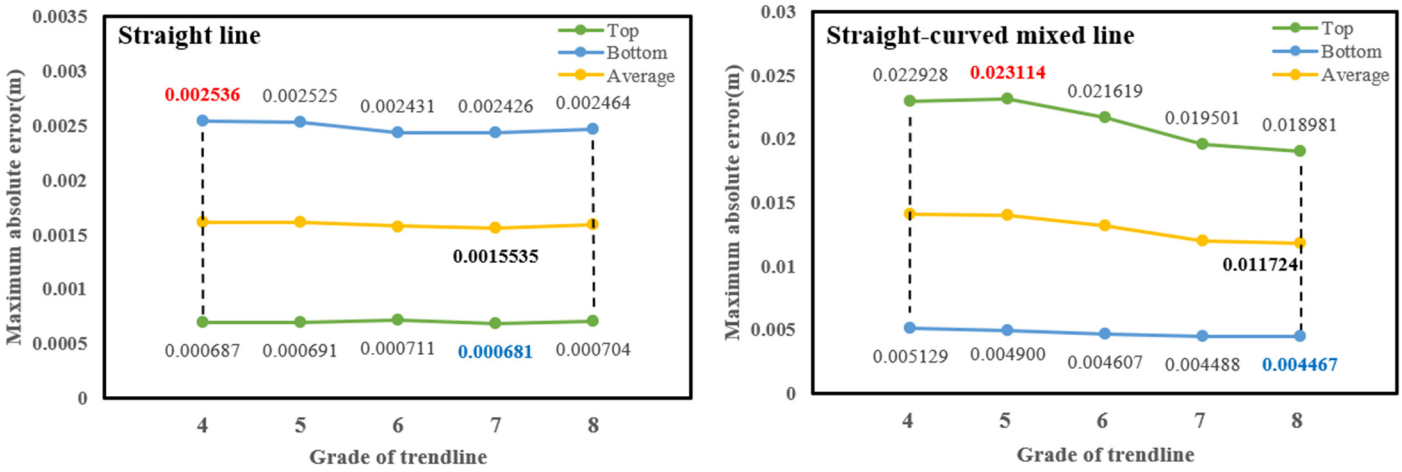

Figure 10. Error values of trend lines compared to actual construction site.

The maximum errors between the actual site drawing and the generated paths are marked in red, while the smallest errors are marked in blue, as confirmed through the algorithm code. In the case of the straight section, the fourth-order trendline path had the maximum error, which was 0.002536 m, a very small value. The minimum error occurred in the seventh-order trendline path, with a value of 0.000681 m, which is approximately 0.002 m smaller than the maximum error.

For the straight–curved mixed section, the maximum error occurred in the fifth-order trendline path, measuring 0.023114 m. Although this value is relatively small, it is about 10 times higher compared to the straight section. The minimum error, observed in the eighth-order trendline path, was 0.004467 m, indicating that even the minimum error in the curved section is larger than the minimum error in the straight section.

The results align with the prediction that straight sections, with minimal changes in slope, would exhibit higher accuracy. While selecting the path with the minimum error is a valid approach, to choose the most accurate path, the average error was calculated by comparing errors in both top and bottom lines. Although it is obvious that the trend line has the least error in general for the straight line section compared to the curved section, the error is still very small for the curved section. This is a positive outcome, as this brings us one step closer to smart construction technology being used in the field.

5. Conclusions

This research offers a methodology for creating efficient work paths for construction rollers, aligning with the growing trend of smart construction technology. This technology is crucial for enhancing overall productivity and worker safety in construction. Using UAVs, the study collected precise, real-time site information quickly. These data help optimize roller routes based on equipment characteristics. Unlike traditional methods

reliant on operator skills, this approach generates optimal paths, making it suitable for construction equipment control systems in smart construction technology.

The research considered factors like redundancy and effective width, extending to curved sections requiring equipment rotation. BIM models incorporated design and roller data, automating planning for improved efficiency. Roller operations typically involve straightforward forward and backward movements, with simple path patterns. Paths were created using the coordinates of the outermost work area line. A case study with actual South Korean road construction drawings revealed a maximum error of approximately 0.002 m for straight sections and 0.02 m for mixed straight–curved sections, with better accuracy in straight-line sections. For sections with changing gradients like curves, adjustments may include higher-order trendlines or narrower coordinate intervals. In essence, this research contributes to smart construction technology by providing a method for optimizing roller paths using UAV data, BIM modeling, and automation to enhance efficiency and accuracy in earthwork operations. In addition, by advancing study on existing path planning, this study provides not only a single route, but multiple paths, similar to actual work paths. Furthermore, it has the advantage of increasing worker convenience and work completeness by calculating or quickly changing the elements necessary for work according to site information.

Construction sites are dynamic environments with various challenges, including avoiding collisions with other equipment and obstacles, which was not addressed in this study. Future research should tackle these dynamic factors. Furthermore, this study concentrated on rollers for path generation, but construction sites involve a mix of equipment like graders and dozers, each with distinct work characteristics. Future research will consider these variations to enhance overall efficiency. This study is considered limited, as it only introduces a theoretical methodology without progressing to linking with actual earthwork equipment. The authors' intention is to pursue ongoing research, extending it to system construction and software development by exploring and applying dynamic factors with the work characteristics outlined earlier. The ultimate goal is to perform a TESTBED and achieve technology for practical use by establishing connections with actual equipment.

Author Contributions: H.-J.K. was responsible for the conceptualization and methodology of the work; J.-Y.K. and J.-W.K. carried out the investigation and participated in writing the manuscript. S.-K.K. supervised the manuscript and W.S.N. supervised and carried out reviewing and editing the manuscript. All authors have read and agreed to the published version of the manuscript.

Funding: This research was funded by the Seoul National University of Science and Technology, grant number 2023-1061.

Institutional Review Board Statement: Not applicable.

Informed Consent Statement: Not applicable.

Data Availability Statement: Data are contained within the article.

Conflicts of Interest: The authors declare no conflicts of interest.

References

1. Park, S.; Kim, J.; Lee, S.; Seo, J. A Comparative Analysis of Automated Machine Guidance and Control Systems for Trench Excavation. *KSCE J. Civ. Eng.* **2021**, *25*, 4065–4074. [CrossRef]
2. Vahdatikhaki, F.; Hammad, A. Risk-based look-ahead workspace generation for earthwork equipment using near real-time simulation. *Autom. Constr.* **2015**, *58*, 207–220. [CrossRef]
3. Vahdatikhaki, F.; Hammad, A.; Langari, S.M. Multi-agent system for improved safety and productivity of earthwork equipment using real-timelocation systems. In Proceedings of the ICSC15: The Canadian Society for Civil Engineering 5th International/11th Construction Specialty Conference, Vancouver, BC, Canada, 7–10 June 2015.
4. Vahdatikhaki, F.; Hammad, A. Dynamic equipment workspace generation for improving earthwork safety using real-time location system. *Adv. Eng. Inform.* **2015**, *29*, 459–471. [CrossRef]
5. Luo, H.; Liu, J.; Fang, W.; Love, P.E.; Yu, Q.; Lu, Z. Real-time smart video surveillance to manage safety: A case study of a transport mega-project. *Adv. Eng. Inform.* **2020**, *45*, 101100. [CrossRef]

6. Zhao, Y.; Zheng, Z.; Liu, Y. Survey on computational-intelligence-based UAV path planning. *Knowl.-Based Syst.* **2018**, *158*, 54–64. [CrossRef]
7. Sonmez, A.; Kocyigit, E.; Kugu, E. Optimal path planning for UAVs using genetic algorithm. In Proceedings of the 2015 International Conference on Unmanned Aircraft Systems (ICUAS), Denver, CO, USA, 9–12 June 2015; pp. 50–55.
8. Roberge, V.; Tarbouchi, M.; Labonté, G. Comparison of parallel genetic algorithm and particle swarm optimization for real-time UAV path planning. *IEEE Trans. Ind. Inform.* **2012**, *9*, 132–141. [CrossRef]
9. Li, G.; Li, Y. UAV path planning based on improved ant colony algorithm. In Proceedings of the Second International Conference on Algorithms, Microchips, and Network Applications (AMNA 2023), Xi'an, China, 8–10 March 2023; pp. 59–63.
10. Aggarwal, S.; Kumar, N. Path planning techniques for unmanned aerial vehicles: A review, solutions, and challenges. *Comput. Commun.* **2020**, *149*, 270–299. [CrossRef]
11. Cho, S.W.; Park, J.H.; Park, H.J.; Kim, S. Multi-uav coverage path planning based on hexagonal grid decomposition in maritime search and rescue. *Mathematics* **2022**, *10*, 83. [CrossRef]
12. Kyriakakis, N.A.; Marinaki, M.; Matsatsinis, N.; Marinakis, Y. A cumulative unmanned aerial vehicle routing problem approach for humanitarian coverage path planning. *Eur. J. Oper. Res.* **2022**, *300*, 992–1004. [CrossRef]
13. Zammit, C.; van Kampen, E.J. Real-time 3D UAV path planning in dynamic environments with uncertainty. *Unmanned Syst.* **2023**, *11*, 203–219. [CrossRef]
14. Kim, S.K.; Jang, J.W.; Na, W.S. Automatic Creation of Heuristic-Based Truck Movement Paths for Construction Equipment Control. *Appl. Sci.* **2021**, *11*, 5837. [CrossRef]
15. Hirayama, M.; Guivant, J.; Katupitiya, J.; Whitty, M. Path planning for autonomous bulldozers. *Mechatronics* **2019**, *58*, 20–38. [CrossRef]
16. Ghadami, N.; Deravian, B.; Pouresmaeil, H.; Aghlmand, R.; Gheibi, M. Smartening the movement path of municipal garbage trucks using genetic algorithm with emphasis on economic-environmental indicators. *Ann. Environ. Sci. Toxicol.* **2021**, *5*, 80–85.
17. Li, R.; Zhou, C.; Dou, Q.; Hu, B. Complete coverage path planning and performance factor analysis for autonomous bulldozer. *J. Field Robot.* **2022**, *39*, 1012–1032. [CrossRef]
18. Shi, M.; Wang, J.; Li, Q.; Cui, B.; Guan, S.; Zeng, T. Accelerated earth-rockfill dam compaction by collaborative operation of unmanned roller fleet. *J. Constr. Eng. Manag.* **2022**, *148*, 04022046. [CrossRef]
19. Zhang, Q.; Liu, T.; Zhang, Z.; Huangfu, Z.; Li, Q.; An, Z. Unmanned rolling compaction system for rockfill materials. *Autom. Constr.* **2019**, *100*, 103–117. [CrossRef]
20. Jang, J.W.; Hyun, J.O.; Kim, S.K. Creation of dozer work plans for C-Map navigation. *Proc. Korean Railr. Soc.* **2022**, *25*, 241–254. [CrossRef]